# Polyol-functionalized thin-film composite membranes with improved transport properties and boron removal in reverse osmosis

# Polyol-functionalized Thin-Film Composite Membranes with Improved Transport Properties and Boron Removal in Reverse Osmosis

M. Di Vincenzo[a,b], M. Barboiu[a], A. Tiraferri[b], Y.M. Legrand[a]

[a]*Institut Européen des Membranes (IEM) UMR5635 (CNRS-ENSCM-Univ.Montpellier) Pl. Eugene Bataillon, F-34095 Montpellier 5, France.*

[b]*Politecnico di Torino, Department of Land, Environment and Infrastructure Engineering (DIATI), Turin, Italy.*

Corresponding author: Y.M. Legrand, yves-marie.legrand@umontpellier.fr

**Abstract**

Thin-film composite membranes comprising modified polyamide layers were cast on an ultrafiltration polysulfone support using sequential interfacial polymerization, thus obtaining bilayer membranes with a final layer of polyols at the surface. A traditional polyamide layer made by interfacial polymerization of trimesoyl chloride and m-phenylene diamine, as well as a reference bilayer membrane with a topmost layer of m-phenylenediamine, were compared with novel bilayer membranes containing N-Methyl-D-glucamine, (±) 3-amino-1,2-propanediol, or serinol functionalizations. Filtration experiments performed with pure water, or with solutions containing 2000 mg/L NaCl and 5 mg/L boric acid, indicated that the water permeance of the modified membranes was improved with no associated loss of salt rejection compared to reference membranes. In particular, functionalization using (±)-3-amino-1,2-propanediol allowed achievement of the highest water flux and the best rejection (NaCl permeance, *B*, of 0.18 L $m^{-2}$ $h^{-1}$) with 40% reduction in salt passage compared to the reference membranes (*B* of 0.26 L $m^{-2}$ $h^{-1}$). Bilayer membranes also showed enhancement in boron removal, performing about 90% observed boron rejection at pH 5.2, condition under which boron is mostly present as neutral boric acid. The strategy employed in the present work allows for robust design of TFC membrane consisting of active layers with improved water permeance and boron rejection performances.

**Keywords**: TFC membranes, water treatment, salt rejection, boron removal, reverse osmosis

**Highlights**:

- Design of novel TFC membranes obtained by sequential interfacial polymerization
- Top layer of polyols allows tuning of surface chemistry and high water permeance
- High selectivity with up to 40% reduction in NaCl passage.
- 90% boron rejection observed at pH 5.2 (neutral form of boric acid)

## 1. Introduction

Currently, the market of high salt rejection membranes for water and wastewater treatment is dominated by thin-film composite (TFC) membranes comprising an active layer of polyamide (PA) made by interfacial polymerization (IP) [1-3]. In particular, IP reaction of *m*-phenylenediamine with trimesoyl chloride gives rise to fully aromatic films, used predominantly for high pressure membrane applications. This procedure allows production of membranes that are currently employed in processes requiring robust water/contaminant separation, such as seawater desalination [2]. However, traditional polyamide membranes suffer from inherent flaws, which reduce their performance during operation [2, 4-7].

Weaknesses of these membranes include surface roughness and the presence of a significant residual amount of terminal carboxyl groups [2, 8, 9]. These characteristics have been related to fouling, caused by attachment of molecules, suspended solids, and microorganisms at the membrane/liquid interface [1, 10, 11]. Also, attempts are ongoing to increase the permeability of polyamide films for water, while maintaining or increasing the removal of ions and other contaminants. Highly efficient membranes have been synthetized by adjusting several parameters during IP, such as the type of monomers, their concentration, the reaction time or other protocol parameters, the type and characteristics of the underlying porous support, or by using additives [5, 6, 12]. Other approaches are based on post-functionalization of polyamide films [7, 13].

In a TFC membrane, each individual layer can be optimized independently and this rationale may be applied to design active layers consisting of more than one barrier film, with each film providing specific properties to improve selectivity or to prevent fouling. Multi-layer TFC membranes were discussed in which amino monomers were made to bind with the unreacted acyl chloride groups after the first IP step, thus creating a second polyamide layer in a further polymerization reaction onto the surface of the first layer [14-16]. Authors highlighted certain

advantages of membranes made with this approach, named sequential interfacial polymerization (SIP), compared to those prepared by conventional IP. This novel approach was adopted to improve rejection of toxic substance (e.g., boron, arsenic), as well as to increase water permeance [14].

In this study, we develop on the SIP methodology to fabricate bilayer membranes for reverse osmosis. A functional topmost separation layer is cast by reacting amino polyols derivatives with the underlying layer of traditional polyamide. These molecules undergo covalent binding with polyamide resulting in the presence of polyol groups at the membrane surface. Three different amino alcohols are used separately and the resulting membranes are characterized. In particular, water permeance, NaCl and boron rejection are measured under low-pressure RO conditions. This work presents a simple method to produce TFC membranes capable to reject salts as well as small neutral contaminants, such as boron, in order to provide effective water treatment.

## 2. Fabrication and characterization of TFC membranes

### 2.1 Materials

Trimesoyl chloride (TMC) 98%, m-phenylediamine (MPD) 99%, sodium chloride (NaCl) ≥ 99.5%, sodium metabisulfite ($Na_2S_2O_5$) ≥ 98%, boric acid ($H_3BO_3$) ≥ 99.5%, sodium hydroxide (NaOH) ≥ 97%, and histamine dihydrochloride 98% were purchased from Sigma-Aldrich. Serinol (SRN) ≥ 98%, (±)-3-amino-1,2-propanediol (APD) 97%, and N-methyl-D-glucamine (GCMN) > 99% were provided by TCI. Chemicals were dissolved in DI (deionized) water or hexane prior to membrane fabrication. DI water was obtained from a Milli-Q purification system. Polysulfone (PSf) ultrafiltration membranes M-PS20-GPET (Nanostone Water, USA) were used as support layers for the fabrication of active thin films.

All the reagents and solvents mentioned above were used without any further purification or anhydrization.

## 2.2 Fabrication of TFC membranes

All the membranes discussed in this study (traditional, reference, and functionalized) were synthesized in our laboratory, unless otherwise mentioned. Several functionalized polyamide (POMPA) layers were prepared on an ultrafiltration PSf support using sequential interfacial polymerization (SIP) (Figure 1). For a comparative study, a reference traditional polyamide membrane and a polyamide bilayer membrane (REFPA) were first synthetized. To fabricate POMPA layers, the second layer was obtained by reaction with amino alcohol molecules, while the REFPA membrane was obtained by second reaction with MPD. The investigated amino alcohols were N-Methyl-D-glucamine, (±) 3-amino-1,2-propanediol, and serinol, and the related membranes are referred to as GCMN, APD, and SRN membrane, respectively.

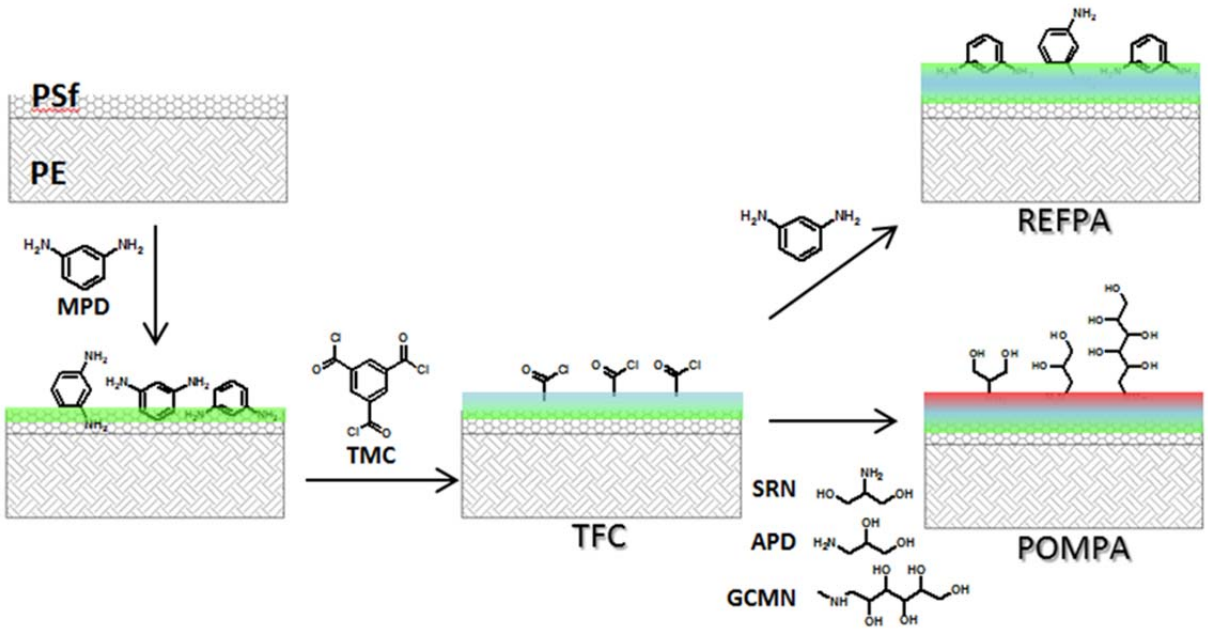


Figure 1. Preparation of modified and reference PA membranes.

### 2.2.1 Fabrication of traditional polyamide membranes

Traditional polyamide active layers were cast on top of commercial PSf support membranes via a traditional IP approach [17]. The support membrane was taped onto a stainless steel plate to leave only the topmost surface available for reaction. It was then placed in a 3.4 wt. % aqueous solution of MPD for 120 seconds. An air gun was used to remove the excess solution from the membrane surface. The membrane was then immersed in a 0.15 wt. % TMC solution (in hexane) for 60 seconds. During this step, the ultra-thin polyamide layer was formed. The composite membrane was then cured in DI water at 95 °C for 120 seconds, rinsed with a 200 ppm NaOCl aqueous solution for 120 seconds, followed by soaking in a 1000 ppm $Na_2S_2O_5$ aqueous solution for 30 seconds and a final wet curing step at 95 °C for 120 seconds in DI water. The TFC membranes were stored in DI water at 4 °C until use.

### 2.2.2 Sequential interfacial polymerization of MPD-TMC-MPD polyamide bilayer membranes (REFPA)

To fabricate reference bilayer membranes, the IP procedure described above was extended by adding one more reaction step. After polyamide formation by IP and before hydrolysis of the unreacted acyl halides, the composite membrane was again immersed in a 3.4 wt. % aqueous MPD solution for 120 seconds to form the second polyamide layer. As amines are more reactive than water, amide formation rate was higher than hydrolysis of the available acyl chloride moieties. Subsequently, unreacted acyl chlorides were rapidly hydrolyzed to carboxyls through reaction with the surrounding water (large excess). The following curing steps were identical to those mentioned for traditional polyamide membranes. These MDP-TMC-MDP membranes are referred to as REFPA. They were fabricated to obtain a better comparison with the functionalized membranes described below, as all of these membranes comprised an additional layer compared to the traditional polyamide films.

### 2.2.3 Sequential interfacial polymerization of novel amino alcohol functionalized polyamide bilayer membranes (POMPA)

The protocol used for the preparation of the functionalized polyamide (POMPA) membrane was similar to that used for REFPA fabrication. However, in this case the first polymerization was followed by an additional step in which the just-formed polyamide layer was contacted with a 0.15 wt. % solution of the corresponding amino alcohol (GCMN, APD, or SRN). Also in this case, amide formation was more favorable than hydrolysis of the available acyl chlorides, as amines are more reactive than water or than alcohol groups. Unreacted acyl chlorides gave then rise to carboxyl moieties upon subsequent hydrolysis. The preparation of the first layer and the subsequent curing steps were analogous to those described above.

## 2.3. Surface properties of the membranes

### 2.3.1. Water contact angles

Hydrophilicity or wettability of the composite membranes was evaluated from contact angle measurements (GBX - Digidrop, Romans, France) by a statistic sessile drop method consisting of measurement of the angle between interfaces of a liquid droplet and a partially wetted solid substrate [18]. The obtained contact angles are shown in Figure 2a. Contact angles measured on traditional polyamide films were consistent with literature values [2]. REFPA membranes were less wettable due to the upper layer obtained by reaction with MPD: MPD is more hydrophobic than TMC, as amine functionalities have lower affinity with water than carboxyls and as this monomer contains lower number of moieties in its structure, i.e., two amines in MPD and three functionalities in TMC. The most significant result apparent from Figure 2a is that all the three novel membranes displaying surface hydroxyl groups had more wettable surfaces than traditional membranes. Specifically, their surface wettability decreased in the order GCMN > ADP ~ SRN. Representative images of the water droplet sitting on these surfaces are shown in Figure S1 of the Supporting Information.

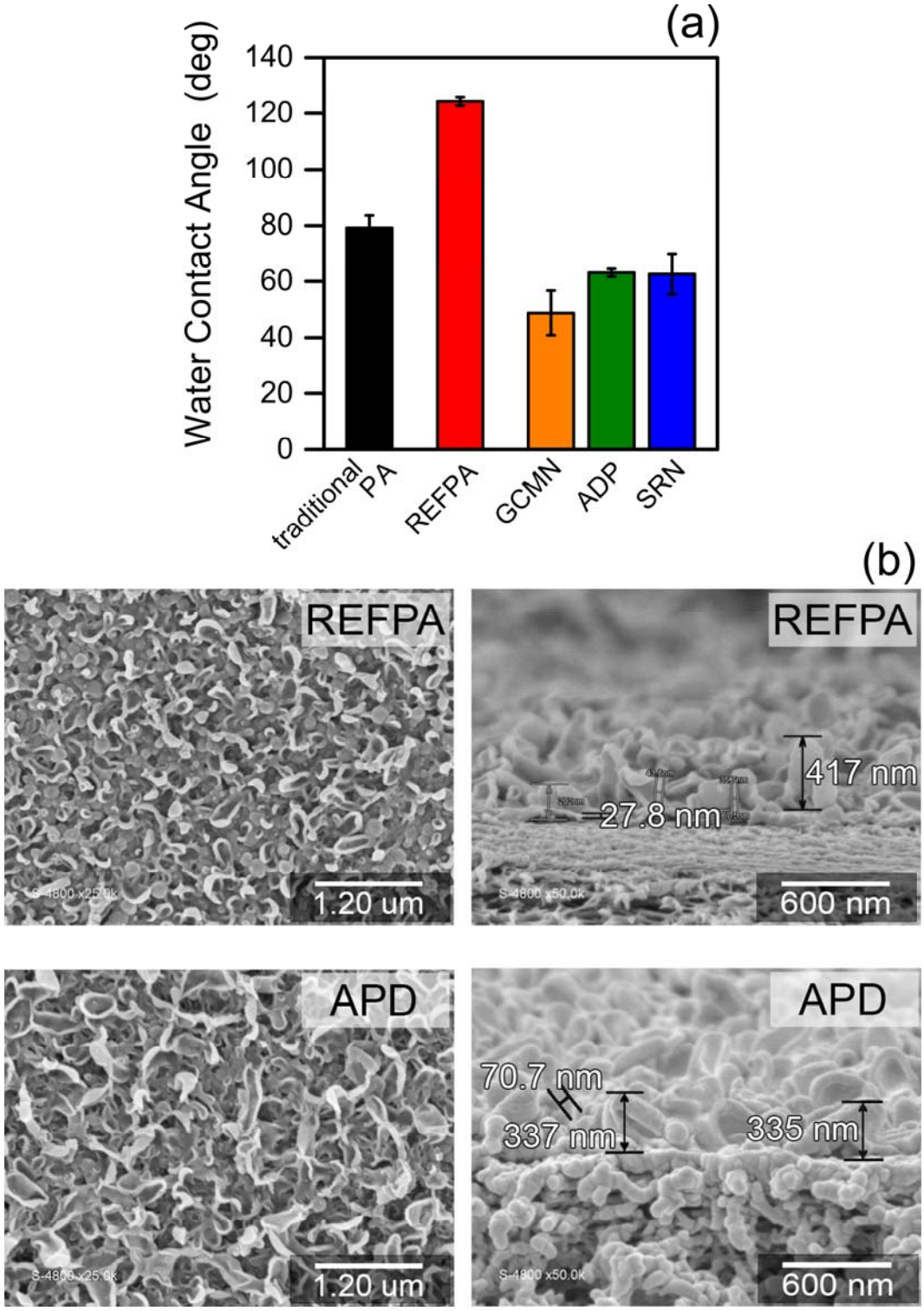


Figure 2. Surface properties of the membranes. (a) Water contact angles (averages and standard deviations) on all the membranes discussed in this study; (b) Representative SEM micrographs of the (left column) cross-section and (right column) surface of (top row) REFPA and (bottom row) ADP membranes.

### 2.3.2. Morphology of the active layers

Top layer surface and cross-section images of each membrane were acquired using a scanning electron microscope (SEM) (Zeiss EVO HD15) coupled with an Oxford X-MaxN EDX detector (Energy-dispersive X-ray spectroscopy analysis and elemental mapping). Figure 2b shows representative SEM micrographs of REFPA and ADP membranes. All POMPA membranes showed a "ridge and valley" conformation, typical of polyamide membranes made by IP of TMC and MPD [2, 3, 16]. This characteristic structure has large roughness and surface area, which contributes to enhanced membrane flux [19].

The overall thickness estimated from SEM images was slightly increased from approximately 200-270 nm for traditional polyamide membranes to roughly 280-360 nm for REFPA and POMPA membranes. This result is consistent with the additional layer formed by SIP. Representative SEM micrographs of TFC, GCMN, and SRN membranes are reported in the SI (Figure S2).

## 2.4. Membrane filtration tests

Water permeance ($A$), NaCl permeance ($B$), and salt rejection of the fabricated membranes were evaluated in a laboratory-scale dead-end filtration system (Sterlitech, model HP4750), with an effective membrane area of 12.56 $cm^2$. Membrane samples were clamped into the dead-end cell, where 25 °C DI water was circulated throughout the feed loop at an applied pressure ($\Delta P$) of 17 bar (246 psi) for 2 h to allow the membrane to equilibrate and the system to reach steady-state (compaction step). Pure water flow was then measured gravimetrically: water flux, $J_W$, was calculated by dividing the flow by the membrane area, while the water permeance, $A$, was calculated by dividing the water flux by the net operating pressure applied across the membrane. Subsequently, 2000 ppm of NaCl were added to the feed, and after allowing the system to reach steady-state conditions, flux and salt rejection were measured by keeping the applied pressure $\Delta P$ at 15 bar (217 psi). NaCl concentrations in the permeate and

in the feed were measured using a conductivity meter and then converting electric conductance into salt concentration via a calibration curve (Figure S3). The observed salt rejection was determined as: $R_o = 1 - \frac{c_p}{c_f}$, where $c_p$ and $c_f$ are the bulk salt concentrations in the permeate and feed solution, respectively. The reported rejection values for each sample are the average of three different measurements, each collected over approximately 30 min. From the observed rejection, the real rejection of the samples, $R_r$, was calculated based on the film model of concentration polarization [1], according to which:

$$\frac{1-R_o}{R_o} = \frac{1-R_r}{R_r} \cdot \exp\left(\frac{J_{W,S}}{k}\right)$$

where $J_{W,S}$ is the permeate flux of the saline solution and $k$ is the mass transfer coefficient of the cell. This coefficient was determined experimentally through the reduction of permeate flux compared to the case of pure water as feed, due to the osmotic pressure prevailing on the membrane surface upon addition of salt, as discussed in previous studies [20]. The NaCl permeance, $B$, was thus determined using the real rejection values [1, 21]:

$$B = J_{W,S}\left(\frac{1-R_r}{R_r}\right)$$

To measure the rejection of boron, a stock solution of boric acid, $H_3BO_3$ (B(III)), was prepared in DI water and added to the feed solution already containing 2000 ppm of NaCl, such that the concentration of boron in the feed solution was 2.5 mg $L^{-1}$ (initial concentration of boric acid: 5 ppm). Boron rejection was determined with the same procedure described above for NaCl. The concentration of boron in the feed and in the permeate samples was determined by inductively coupled plasma with mass spectrometry (ICP-MS). This discussion reports values of the apparent boron rejection ($BR_o$) quantified using the analogous equation

described earlier to calculate observed NaCl rejection: $BR_o = \left(1 - \frac{C_{Bp}}{C_{Bf}}\right)$, where $c_{Bp}$ and $c_{Bf}$ are the boron concentrations of the permeate and feed solution, respectively.

## 3. Separation performance of functionalized membranes

Results of filtration tests showed that the reference bilayer membranes (REFPA) prepared for comparative studies had very similar separation performances to traditional polyamide membranes, although constituted of an extra thin layer of polyamide (MPD-TMC-MPD). This 3-component REFPA membrane represents a better comparison with the 3-components POMPA membranes than the traditional polyamide films. Water permeance, NaCl rejection, and the resulting value of the NaCl permeances for the different membranes fabricated for this study are summarized in Table 1 (individual values for all samples are presented in Table S1 of the Supporting Information).

Table 1. Permeances and NaCl rejections of the membranes.

| Membrane | Water permeance (A) [LMH/bar] | Observed NaCl rejection (R) [%] | Real NaCl rejection ($R_r$) [%] | NaCl permeance (B) [LMH] |
|---|---|---|---|---|
| **PA** | 1.09 ± 0.13 | 95.3 ± 0.77 | 99.3 ± 0.15 | 0.23 ± 0.04 |
| **REFPA** | 1.03 ± 0.04 | 94.7 ± 0.43 | 99.0 ± 0.06 | 0.26 ± 0.02 |
| **GCMN** | 1.81 ± 0.18 | 92.7 ± 0.61 | 98.9 ± 0.08 | 0.37 ± 0.03 |
| **APD** | 1.79 ± 0.28 | 96.2 ± 0.10 | 99.4 ± 0.03 | 0.18 ± 0.01 |
| **SRN** | 1.46 ± 0.10 | 92.6 ± 0.61 | 98.4 ± 0.09 | 0.37 ± 0.03 |

### 3.1 Water Permeance

Water permeance values were consistent with literature reports of TFC polyamide membranes [4, 6]. All the POMPA films modified using hydrophilic molecules had consistently higher water permeance compared to membranes consisting of traditional polyamide layers and compared to reference REFPA membranes; see Figure 3. Specifically, fluxes increased in the order REFPA < SRN < ADP ~ GCMN. Therefore, the APD and the GCMN membranes showed the best increase in water permeance, reaching roughly 1.8 LMH/bar, which represents an increase of approximately 75% compared to the REFPA membranes. SRN-POMPA membranes showed slightly lower permeance values (1.46 LMH/bar). These improvements may partly be explained with differences in wettability (presence of hydroxyl groups –OH) [22]. Indeed, while the water contact angle on REFPA surface was on average 124°, the angles were 63.1° and 48.8° for ADP and GCMN, respectively. If hydrophilicity was the only criteria for higher water permeance, the permeance of traditional polyamide and REFPA membranes should also be quite different, given the observed water contact angle (79.2° and 124°, respectively). However, the *A* values for these two reference membranes were very close, within 6%. One possible interpretation is that, from the molecular point of view, the functionalization with the amino alcohols may present a slightly more *open* interface between the bulk solution and the inner membrane, as depicted in Figure 3. In this case, the loss in entropy might be compensated by a hydrophilic funneling effect helping the water molecules to cross the hydrophobic barrier (MPD and TMC monomers contain hydrophobic benzyl rings while polyols do not contain such moiety) [23].

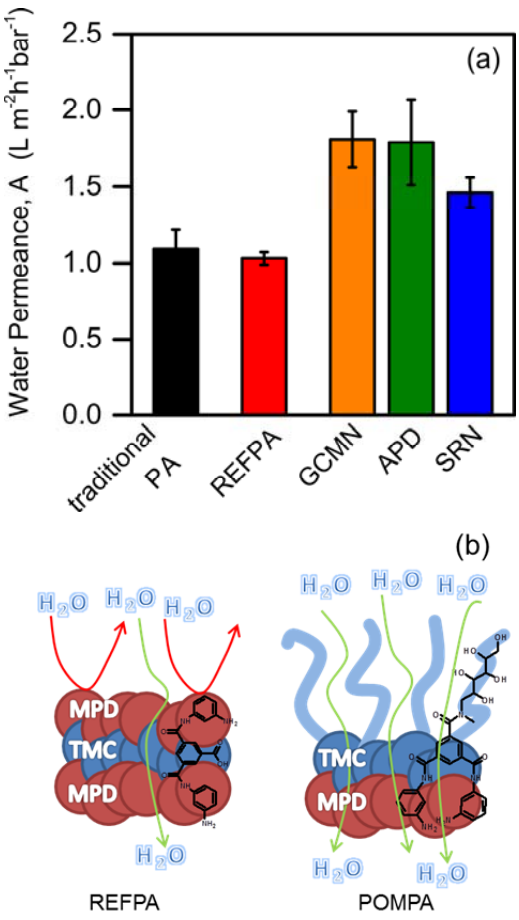


Figure 3. (a) Water permeance of all the membranes discussed in this study and (b) schematic representation of the liquid-solid interface of the TFC membranes. In the case of POMPA, the water molecules are dragged from the bulk solution to the membrane through the hydroxyl moieties of the alcohol derivatives [24, 25].

### 3.2. Salt rejection

The functionalization performed in this study improved the water permeance of membranes significantly without impairing their rejection capabilities. When comparing the real rejection listed in Table 1, this parameter increased following the sequence: SRN < GCMN < REFPA < APD. Functionalization using (±)-3-amino-1,2-propanediol (APD) allowed achievement of the best selectivity, with 0.4% higher salt rejection compared to REFPA (99.0% for REFPA and 99.4% for ADP), which corresponds to a 40% reduction in salt passage, while for all the other membranes, the results consistently showed real salt rejection value in the range of 98.4-

99.3%. The average salt rejection and permeance values of APD membranes are statistically different to those of SNR and GCMN membranes, based on t-tests performed with a significance level of 5%.

The performances of the novel amino alcohol functionalized membranes were also compared with literature values [14]. Figure 4 shows salt passage values of all the membranes fabricated in this study plotted as a function of water permeance on the base-comparative-graph of commercial seawater reverse osmosis membranes (see Table S1 for values of individual samples). This graph allows appreciation of the typical permeability-selectivity trade-off of polyamide films characterized by solution-diffusion transport. The dash line represents the experimental upper boundary as already reported by other authors (left, Figure 4) [26]. Eleven data points were plotted in the base-comparative-graph, showing that all the membranes performed in the range of the commercially available ones. Data points relative to APD membranes lie in the upper right part of the graph, implying high water permeance coupled with low salt passage (see zoomed view on the right of Figure 4). The enhanced performance exhibited by APD membrane may be explained by the combined effect of (i) retained critical pore size and density, (ii) the more wettable surface nature thanks to the new functional hydroxyl groups at the top layer, and (iii) the funneling effect discussed above. However, our results suggest that an additional monomeric layer does not necessarily yield an enhancement in salt rejection.

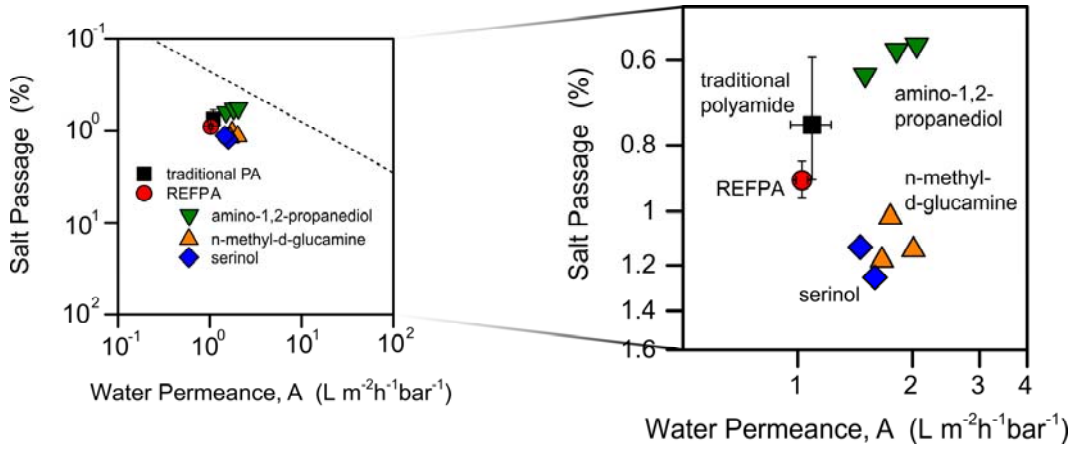


Figure 4. Experimental water permeance and NaCl passage of the membranes plotted on a base-comparative-graph; (left) data points in comparison with the trade-off upper boundary depicted as a dash line [26]; (right) zoomed-in view of the data points collected in this study. Data points for traditional polyamide and REFPA membranes (black square and red circle, respectively) are averages for different samples showing standard deviations. Individual values of each sample are instead presented for POMPA amino alcohol membranes.

### 3.3. Boron rejection

The separation performance of the POMPA membranes was also evaluated for a small neutral and potentially toxic molecule, namely boric acid (5 ppm) in presence of NaCl (2000 ppm), in order to simulate brackish water conditions and to verify boron rejection. Indeed, boron concentration in seawater is around 4.5 mg $L^{-1}$ [27]. The limit set for boron by regulation agencies can be as low as 0.5 mg $L^{-1}$ and its rejection is strongly dependent on pH [28], increasing from around 50-75% at pH 7-8 to over 95% at pH 10.5. This phenomenon is mainly due to the increased proportion of borate ions at higher pH, which facilitates rejection (charged ions are hydrated and thus larger than neutral ions) [27-29]. However, increasing the pH is often unfeasible in practical operations because of the need to add chemicals, complications to the overall process and flow management, and increased costs [29].

In a thorough comparative previous study, commercial membranes used in the pristine form or modified to improve selectivity showed at best 85% boron rejection within the seawater range (A < 2 LMH/bar) at pH 7 [30, 31]. To our knowledge, the best results at near neutral pH

were obtained by Freeman and colleagues [14]. They showed an enhancement in boron rejection using a hexafluoroalcohol (HFA) polyamide layer cast on top of a traditional polyamide membrane. By increasing the pH from 6.5 to 9.5, these authors observed increased boron rejection from 81.6 to 92.5% and from 84.1% to 94.2% for traditional and functional bilayer membranes, respectively. Therefore, the improvement in boron rejection was due to the enhanced dissociation at pH above the pK of boric acid, i.e., 9.3 [31].

In our experiments, traditional polyamide, REFPA, APD, GCMN, and SRN membranes were challenged with boric acid at an applied pressure of 15 bars, at pH 5.2 and in the presence of NaCl (2000 ppm). Under these conditions, boron was present almost exclusively as neutral boric acid, given its pK of 9.3. Inductively Coupled Plasma Mass Spectrometry (ICP-MS) was used to analyze the boron rejection for all the membranes fabricated in this study and presented in Table 2. Our results showed consistent observed rejection of boron at values of roughly 90% for all membranes except those modified with serinol, for which boron rejection was lower. The initial concentration of boric acid being 5 ppm, the final concentration in the permeate was in the range of 0.45 mg/L. These rejection values are significantly higher than those presented by other authors for similar membranes fabricated at laboratory scale for pH values of the feed below 9.5 [14, 30].

The presence of boron on the membrane surfaces following the boron rejection tests was also confirmed by Energy Dispersive X-Ray Spectrometry (EDX) (Figure S4 of the Supporting Information). Boric acid – carbohydrate interactions are well known [32]; although a stronger complex is formed at basic pH than at acidic pH, equilibrium between the boric acid and the borate ester is present. While such experimental evaluation was not performed in this work, it has recently been well documented, including for membranes [33, 34]. The residence time of boron on each binding site may be a reasonable explanation for the boron rejection. As previously demonstrated, subtle diol-ligand structure can reveal significant changes in

properties [35]. The mechanism of adsorption is consistent with the results obtained for the POMPA membranes: when the ethylene glycol motif is not present (SRN), the boron rejection was modest (62%), while it was high (~90%) for the other two functionalization agents (GCMN and APD). All POMPA membranes displayed improved water permeance compare to both TFC and REFPA membranes, thanks to higher hydrophilicity and a "more opened" top layer. The SRN membrane presenting the lowest rejections (especially for boron) does not display the ethylene glycol motif that may thus be critical for achieving simultaneous high water permeance and efficient rejections of salt and, most importantly, boron. In summary, two of the polyol-functionalized membranes (GCMN and ADP) guaranteed high boron rejection while improving other transport properties related to water permeance and NaCl rejection.

Table2. Observed boron rejection (as %, averages and standard deviations) at pH 5.2 for all the membranes fabricated and discussed in this study. TFC and REFPA membranes give in our hands slightly higher boron rejection than previously reported [14] at pH = 9.2 and comparable with GCMN and ADP membranes, which present larger water permeabilties.

| **Membrane** | **Average observed boron rejection** | **Standard deviation** |
|---|---|---|
| | **[%]** | **[%]** |
| **Traditional PA** | 90.6 | 0.70 |
| **REFPA** | 91.4 | 1.01 |
| **GCMN** | 89.0 | 2.40 |
| **APD** | 89.0 | 0.78 |
| **SRN** | 62.0 | 0.57 |

## 4. Conclusions

Bilayers thin-film composite membranes were prepared on a commercial ultrafiltration polysulfone support using sequential interfacial polymerization. These films consisted of a selective layer fabricated using commercially available and cheap N-methyl-D-glucamine, (±)-3-amino-1,2-propanediol, or serinol, cast on top of a traditional polyamide layer. The functionalized membranes were more wettable than reference membranes thanks to the presence of alcohol groups at the surface. They showed consistent higher water permeance than reference membranes, possibly thanks to the combined effect of larger wettability and a structure more prone to the passage of water molecules. The polyol-functionalized membranes also achieved better rejection performance ($B$ = 0.18 LMH) compared to traditional ($B$ = 0.23 LMH) and reference ($B$ = 0.26 LMH) polyamide membranes, with 40% reduction in salt passage, and maintained consistently high boron rejection at low pH (5.2). In particular, the amino alcohol bilayer films showed boron removal in the range of 90% by using the typical seawater feed concentration of 4.5-5 ppm boric acid. The final concentration in the permeate was approximately 0.45 mg/L, below the limit imposed by the WHO for boron in drinking water. In our work, the SIP process itself did not bring significant improvement compared to traditional PA films preparation. Indeed, REFPA membranes prepared by SIP showed lower water permeance than membranes synthesized via the traditional route. Therefore, POMPA membrane property improvements clearly came from the addition of amino alcohols. Although not tested in this study, rejection of boron is expected to be higher at typical seawater pH (~ 7.5-8.5), whereby boric acid is partly ionized, thus more easily rejected by polyamide-based films. Among the various polyols investigated in this study, 3-amino-1,2-propanediol allowed the achievement of the best transport properties. As boron may interact with the alcohol groups exposed at the membrane surface, future work will aim at testing the possible boron accumulation within the membrane and saturation of the interaction sites. Also, the fouling resistance behavior of the polyols-

functionalized membranes should be investigated: these materials do not display carboxylic moieties at their surface, which often act as anchoring points for the attachment of organic acids and carboxyl-rich molecules in the presence of divalent cations. Therefore, organic fouling is expected to be lower than with typical polyamide films.

**Acknowledgments**

This work was financially supported by the DYNMULTIREC (13-IS07-0002-01) ANR program and Politecnico di Torino (58_RIL16TIRLAB). The authors would also like to thank S. Cerneaux and A. Cristian for useful discussions and support, T. Thamy for contact angle measurements and B. Rebière for SEM/EDX analysis.

**Nomenclature**

***Acronyms***

ADP: (±)-3-amino-1,2-propanediol

POMPA: functionalized polyamide; novel bilayer membranes with topmost layer of amino alcohol

GCMN: N-methyl-D-glucamine

IP: interfacial polymerization

MPD: m-phenylediamine

PA: polyamide

PSf: polysulfone

REFPA: reference polyamide; bilayer membranes with topmost layer of MPD

SIP: sequential interfacial polymerization

SRN: serinol

TMC: trimesoyl chloride

TFC: thin-film composite

**Supporting Information**

Representative images of water droplet sitting on all the fabricated membranes; Representative SEM micrographs of traditional PA, GCMN, SRN, and REFPA membranes; Calibration line of conductivity meter; Summarizing table of water permeance and salt rejection values for individual samples; Representative EDX plot and elemental analysis for a GCMN membrane following filtration with boron.

# References


[1] R. Baker, Membrane Technology and Applications, 2nd edition ed., Wiley, 2004.
[2] M. Elimelech, W.A. Phillip, The Future of Seawater Desalination: Energy, Technology, and the Environment, Science 333 (2011) 712-717.
[3] R.J. Petersen, Composite Reverse-Osmosis and Nanofiltration Membranes, J. Membr. Sci. 83 (1993) 81-150.
[4] G.D. Kang, Y.M. Cao, Development of antifouling reverse osmosis membranes for water treatment: A review, Water Res. 46 (2012) 584-600.
[5] W.J. Lau, A.F. Ismail, N. Misdan, M.A. Kassim, A recent progress in thin film composite membrane: A review, Desalination 287 (2012) 190-199.
[6] K.P. Lee, T.C. Arnot, D. Mattia, A review of reverse osmosis membrane materials for desalination-Development to date and future potential, J. Membr. Sci. 370 (2011) 1-22.
[7] J.R. Werber, C.O. Osuji, M. Elimelech, Materials for next-generation desalination and water purification membranes, Nat. Rev. mater. 1 (2016) 16018.
[8] Y.H. Mo, A. Tiraferri, N.Y. Yip, A. Adout, X. Huang, M. Elimelech, Improved Antifouling Properties of Polyamide Nanofiltration Membranes by Reducing the Density of Surface Carboxyl Groups, Environ. Sci. Technol. 46 (2012) 13253-13261.
[9] A. Tiraferri, M. Elimelech, Direct quantification of negatively charged functional groups on membrane surfaces, J Membrane Sci 389 (2012) 499-508.
[10] W.S. Ang, A. Tiraferri, K.L. Chen, M. Elimelech, Fouling and cleaning of RO membranes fouled by mixtures of organic foulants simulating wastewater effluent, J. Membr. Sci. 376 (2011) 196-206.
[11] D. Rana, T. Matsuura, Surface modifications for antifouling membranes, Chem. Rev. 110 (2010) 2448-2471.
[12] A. Giwa, N. Akther, V. Dufour, S.W. Hasan, A critical review on recent polymeric and nano-enhanced membranes for reverse osmosis, RSC. Adv. 6 (2016) 8134-8163.
[13] A. Tiraferri, C.D. Vecitis, M. Elimelech, Covalent Binding of Single-Walled Carbon Nanotubes to Polyamide Membranes for Antimicrobial Surface Properties, ACS Appl. Mater. Inter. 3 (2011) 2869-2877.
[14] Y.H. La, J. Diep, R. Al-Rasheed, D. Miller, L. Krupp, G.M. Geise, A. Vora, B. Davis, M. Nassar, B.D. Freeman, M. McNeil, G. Dubois, Enhanced desalination performance of polyamide bi-layer membranes prepared by sequential interfacial polymerization, J Membrane Sci 437 (2013) 33-39.
[15] Y.-H. La, J. Diep, R. Al-Rasheed, M. Nassar, E.I. Mouhoumed, A. Szymczyk, G. Dubois, The effect of cross-contamination in the sequential interfacial polymerization on the RO performance of polyamide bilayer membranes, J. Membr. Sci. 466 (2014) 348-356.
[16] H. Zou, Y. Jin, J. Yang, H. Dai, X. Yu, J. Xu, Synthesis and characterization of thin film composite reverse osmosis membranes via novel interfacial polymerization approach, Sep. Purif. Technol. 72 (2010) 256-262.
[17] A. Tiraferri, N.Y. Yip, W.A. Phillip, J.D. Schiffman, M. Elimelech, Relating performance of thin-film composite forward osmosis membranes to support layer formation and structure, J. Membr. Sci. 367 (2011) 340-352.
[18] G. Hurwitz, G.R. Guillen, E.M.V. Hoek, Probing polyamide membrane surface charge, zeta potential, wettability, and hydrophilicity with contact angle measurements, J. Membr. Sci. 349 (2010) 349-357.
[19] S.-Y. Kwak, S.G. Jung, S.H. Kim, Structure-motion-performance relationship of flux-enhanced reverse osmosis (RO) membranes composed of aromatic polyamide thin films, Environ. Sci. Technol. 35 (2001) 4334-4340.

[20] I. Sutzkover, D. Hasson, R. Semiat, Simple technique for measuring the concentration polarization level in a reverse osmosis system, Desalination 131 (2000) 117-127.
[21] J. Mulder, Basic principles of membrane technology, Springer Science & Business Media, 2012.
[22] J.T. Arena, B. McCloskey, B.D. Freeman, J.R. McCutcheon, Surface modification of thin film composite membrane support layers with polydopamine: enabling use of reverse osmosis membranes in pressure retarded osmosis, J. Membr. Sci. 375 (2011) 55-62.
[23] M.A. Henderson, The interaction of water with solid surfaces: fundamental aspects revisited, Surf. Sci. Rep. 46 (2002) 1-308.
[24] X. Yao, Y.L. Song, L. Jiang, Applications of Bio-Inspired Special Wettable Surfaces, Adv. Mater. 23 (2011) 719-734.
[25] Y. Zhang, M. Barboiu, Dynameric asymmetric membranes for directional water transport, Chem. Commun. 51 (2015) 15925-15927.
[26] G.M. Geise, H.B. Park, A.C. Sagle, B.D. Freeman, J.E. McGrath, Water permeability and water/salt selectivity tradeoff in polymers for desalination, J. Membr. Sci. 369 (2011) 130-138.
[27] N. Hilal, G.J. Kim, C. Somerfield, Boron removal from saline water: A comprehensive review, Desalination 273 (2011) 23-35.
[28] K.L. Tu, L.D. Nghiem, A.R. Chivas, Coupling effects of feed solution pH and ionic strength on the rejection of boron by NF/RO membranes, Chem. Eng. J. 168 (2011) 700-706.
[29] V.S. Freger, H. Shemer, A.A. Sagiv, R.R. Semiat, Boron Removal Using Membranes, Boron Sep. Process. (2015) 199.
[30] R. Bernstein, S. Belfer, V. Freger, Toward Improved Boron Removal in RO by Membrane Modification: Feasibility and Challenges, Environ Sci Technol 45 (2011) 3613-3620.
[31] E. Guler, C. Kaya, N. Kabay, M. Arda, Boron removal from seawater: State-of-the-art review, Desalination 356 (2015) 85-93.
[32] X. Wu, Z. Li, X.X. Chen, J.S. Fossey, T.D. James, Y.B. Jiang, Selective sensing of saccharides using simple boronic acids and their aggregates, Chem Soc Rev 42 (2013) 8032-8048.
[33] J.Q. Meng, J.J. Cao, R.S. Xu, Z. Wang, R.B. Sun, Hyperbranched grafting enabling simultaneous enhancement of the boric acid uptake and the adsorption rate of a complexing membrane, J Mater Chem A 4 (2016) 11656-11665.
[34] Q. Shi, J.Q. Meng, R.S. Xu, X.L. Du, Y.F. Zhang, Synthesis of hydrophilic polysulfone membranes having antifouling and boron adsorption properties via blending with an amphiphilic graft glycopolymer, J Membrane Sci 444 (2013) 50-59.
[35] X.L. Du, J.Q. Meng, R.S. Xu, Q. Shi, Y.F. Zhang, Polyol-grafted polysulfone membranes for boron removal: Effects of the ligand structure, J Membrane Sci 476 (2015) 205-215.

# SUPPORTING INFORMATION

# Polyol-functionalized Thin-Film Composite Membranes with Improved Transport Properties and Boron Removal in Reverse Osmosis

M. Di Vincenzo[a,b], M. Barboiu[a], A. Tiraferri[b], Y.M. Legrand[a]

[a]*Institut Européen des Membranes (IEM) UMR5635 (CNRS-ENSCM-Univ.Montpellier) Pl. Eugene Bataillon, F-34095 Montpellier 5, France.*

[b]*Politecnico di Torino, Department of Land, Environment and Infrastructure Engineering (DIATI), Turin, Italy.*

Corresponding author: Y.M. Legrand, yves-marie.legrand@umontpellier.fr

## DESCRIPTION OF SUPPORTING INFORMATION

**Figure S1. Representative images of water droplets sitting on all fabricated membranes**

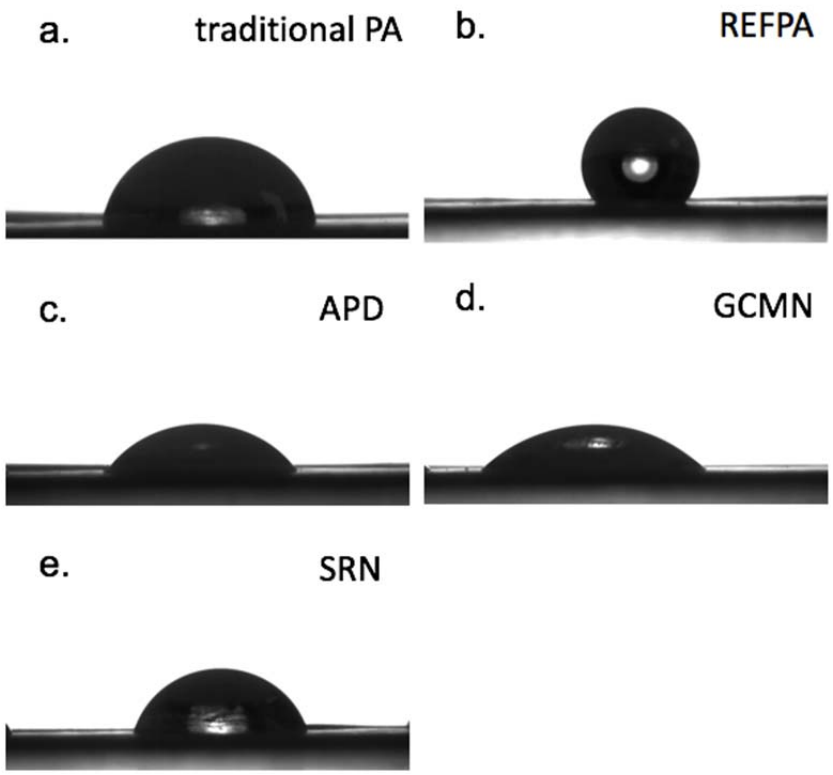


Figure S1. Representative images of water droplets sitting on a: **a.** traditional PA layer (79,2°) – **b.** REFPA membrane – **c.** APD membrane – **d.** GCMN membrane, and – **e.** SRN membrane. Contact angles were measured using a water drop volume of 3 μL, at room temperature of 25°C. Multiple locations on three independent samples were tested in order to average out errors that occur due to roughness and chemical heterogeneity: these averages are presented in the main manuscript. The traditional PA layer exhibited typical value reported in the literature (≅ 80°). APD, GCMN and SRN (FUNPA membranes) showed improved wettability, in accordance with the nature of the functionalized layers and the investigated water permeance.

**Figure S2. Representative SEM micrographs of traditional PA, GCMN, and SRN membranes**

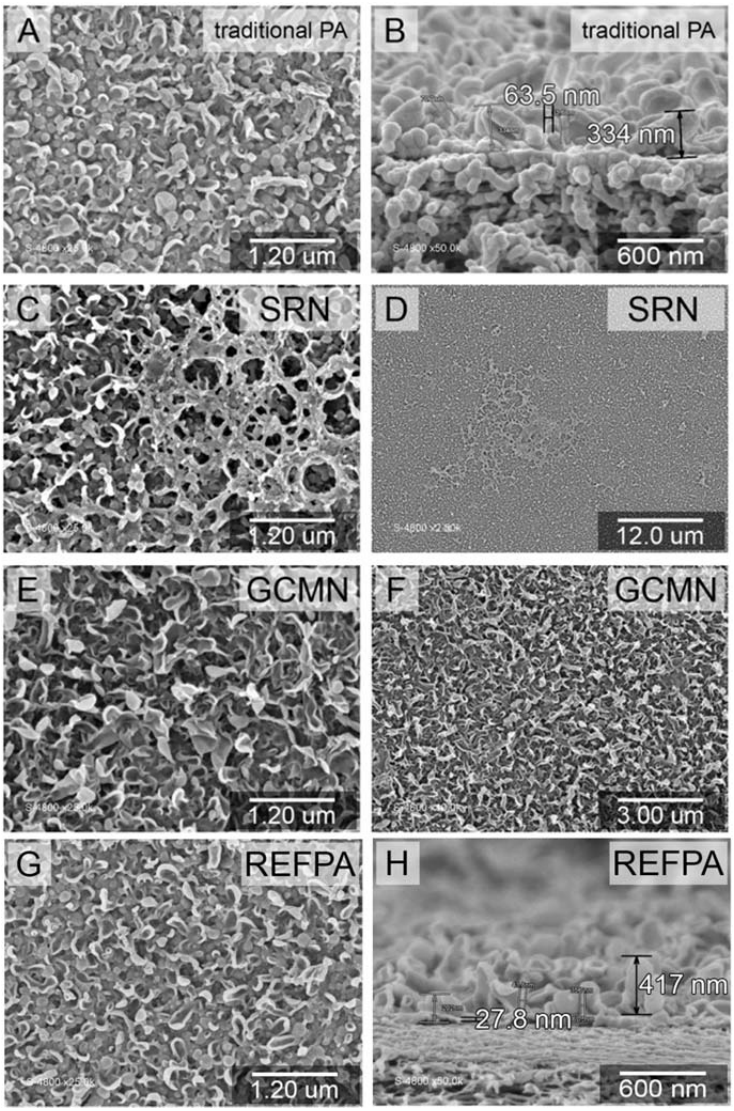


Figure S2. Representative SEM micrographs of (A, B) traditional PA, (C, D) SRN, and (E, F) GCMN, and (G, H) REFPA membranes. Surface images show the typical "ridge and valley" conformation. The thickness of traditional PA is about 350 nm, with a minimum value around 60 nm.

**Figure S4. Calibration curve of conductivity meter**

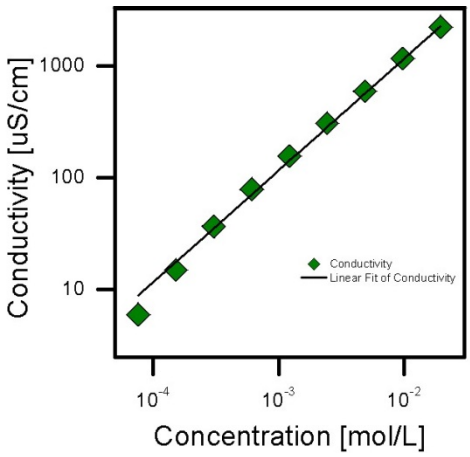


Figure S3. Calibration curve of electrical conductivity meter showing linear correlation with NaCl concentration (log-log plot).

**Table S1. Summarizing table of water permeance (A), observed and real NaCl rejection (R, Rr), NaCl permeance (B), and NaCl passage of individual samples**. Table reports averages and standard deviations (STD) for all the fabricated membranes. Results exhibited a consistent improvement in water permeance for the FUNPA membranes showing an increase of 41%, 73% and 75% for SRN, APD, and GCMN, respectively, compared to reference membranes. All the membranes showed a Rr value of roughly 99%. APD membranes allowed achievement of the best selectivity exhibiting a 40% reduction in NaCl passage.

| | Permeance A | Observed Rejection R | Real Rejection Rr | B | Salt Passage |
|---|---|---|---|---|---|
| | [Lmh/bar] | [%] | [%] | [Lmh] | [%] |
| **TFC1** | 1.11 | 96.25 | 99.43 | 0.180 | 0.57 |
| **TFC2** | 1.08 | 96.17 | 99.27 | 0.237 | 0.73 |
| **TFC3** | 1.23 | 95.47 | 99.28 | 0.223 | 0.72 |
| **TFC4** | 1.16 | 95.24 | 99.28 | 0.234 | 0.72 |
| **TFC5** | 0.88 | 94.37 | 99.01 | 0.279 | 0.99 |
| **REFPA1** | 1.00 | 94.14 | 99.02 | 0.290 | 0.98 |
| **REFPA2** | 0.98 | 95.25 | 99.08 | 0.231 | 0.92 |
| **REFPA3** | 1.06 | 94.59 | 99.11 | 0.266 | 0.89 |
| **REFPA4** | 1.04 | 95.05 | 99.17 | 0.245 | 0.83 |
| **REFPA5** | 1.05 | 94.73 | 99.12 | 0.259 | 0.88 |
| **GCMN1** | 1.75 | 93.38 | 98.98 | 0.327 | 1.02 |
| **GCMN2** | 2.01 | 92.33 | 98.86 | 0.387 | 1.14 |
| **GCMN3** | 1.66 | 92.32 | 98.82 | 0.386 | 1.18 |
| **ADP1** | 1.50 | 96.08 | 99.37 | 0.189 | 0.63 |
| **ADP2** | 1.82 | 96.27 | 99.42 | 0.180 | 0.58 |
| **ADP3** | 2.05 | 96.24 | 99.43 | 0.182 | 0.57 |
| **SRN1** | 1.59 | 92.15 | 98.75 | 0.394 | 1.25 |
| **SRN2** | 1.46 | 93.01 | 98.87 | 0.349 | 1.13 |

**Table S2. Summarizing table of boron rejection data for individual membrane samples**. Boron rejection was investigated at pH 5.2 in the presence of 2000 ppm NaCl.

| Membrane | Measured boron permeate concentration [ppm] | Boron observed rejection [%] | AVERAGE BR [%] | Standard deviation [%] |
|---|---|---|---|---|
| **TFC1** | 0.221 | 91.4 | | |
| **TFC2** | 0.250 | 90.3 | 90.6 | 0.70 |
| **TFC3** | 0.255 | 90.1 | | |
| **REFPA1** | 0.200 | 92.3 | | |
| **REFPA2** | 0.250 | 90.3 | 91.4 | 1.01 |
| **REFPA3** | 0.217 | 91.6 | | |
| **GCMN1** | 0.241 | 90.7 | 89.0 | 2.40 |
| **GCMN2** | 0.330 | 87.3 | | |
| **APD1** | 0.270 | 89.5 | 89.0 | 0.78 |
| **APD2** | 0.299 | 88.4 | | |
| **SRN1** | 0.997 | 61.6 | 62.0 | 0.57 |
| **SRN2** | 0.971 | 62.4 | | |

**Figure S4. Representative EDX plot and table for a GCMN membrane following filtration with boron.**

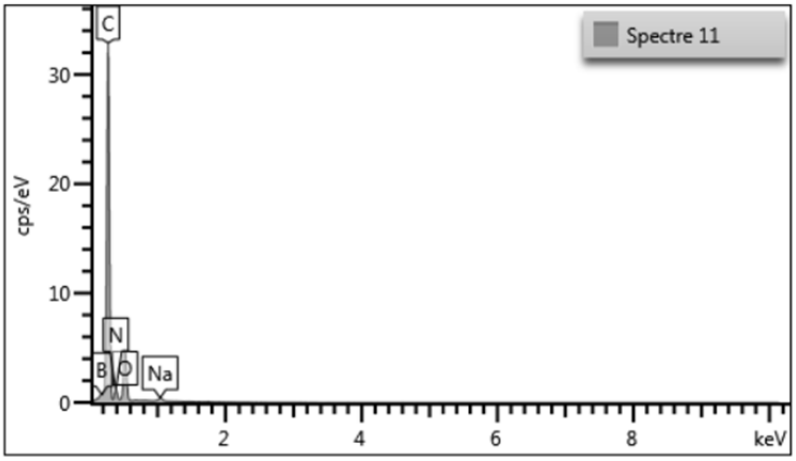


| Élément | % Masse | % atomique |
|---|---|---|
| B | 4.17 | 4.87 |
| C | 71.42 | 75.16 |
| N | 7.69 | 6.94 |
| O | 15.97 | 12.62 |
| Na | 0.75 | 0.41 |
| Total: | 100.00 | 100.00 |

Figure S4. Representative EDX plot elemental analysis for a GCMN membrane following filtration with boron. The data for the other membrane (PA, REFPA, APD and SRN) was not shown as no relevant differences could be observed.